

The Non-adiabatic stereodynamics study for the reaction of $\text{Na}(3s)+\text{H}_2 \rightarrow \text{NaH}(\text{X}^1\Sigma^+)+\text{H}$

Dahai Cheng, Jiuchuang Yuan and Maodu Chen*

*Key Laboratory of Materials Modification by Laser, Electron, and Ion Beams
(Ministry of Education), School of Physics and Optoelectronic Technology,
Dalian University of Technology, Dalian 116024, P.R. China*

Received 13 February 2016; Accepted (in revised version) 20 April 2016
Published Online 25 May 2016

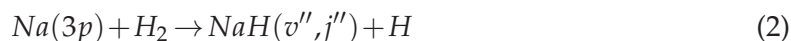
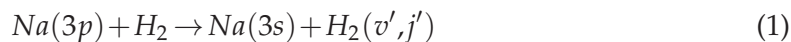
Abstract. A theoretical investigation of the non-adiabatic dynamics processes for the reaction $\text{Na}(3s) + \text{H}_2 \rightarrow \text{NaH}(\text{X}^1\Sigma^+) + \text{H}$ has been performed using the method of coherence switching with decay of mixing (CSDM). The integral cross sections calculated by the CSDM method are compared with the results from an adiabatic quasiclassical trajectory (QCT) calculation, which uses the same potential energy in the adiabatic representation. The product rotational polarization in non-adiabatic dynamics is presented and compared with the adiabatic results by means of the joint distributions of rotational angular momentum vectors in the scattering coordinate. It is found that the conical intersection shows significant influence on the integral cross sections of the reaction. The adiabatic effect also reduces the rotational polarization of the product NaH.

PACS: 34.35.+a, 34.50.-s, 31.50.Gh

Key words: non-adiabatic, stereodynamics, polarization.

1 Introduction

NaH_2 is a prototypical system for metal reactions with covalent molecules, and it has been widely studied experimentally and theoretically in many reactive or non-reactive processes. The reactions:



are often studied as examples of the fundamental processes of electronic-to-vibrational-and-rotational energy transfer (E-VRT) and chemical reaction with an conical intersection

*Corresponding author. *Email address:* mdchen@dlut.edu.cn (M. D. Chen)

in potential energy surface [1]. The E-VRT processes may play significant role in the photochemistry of the earth's atmosphere and are of potential interest in laser chemistry. On the other hand, reactive collisions which involve transitions between different electronic states are prerequisite to a theoretical treatment of any of the more complex photochemical processes.

Most early studies for this system focus on the quenching process in reaction (1), since the energy of the conical intersection is nearly equal to the energy of the Na (3p) asymptote when NaH₂ is in C_{2v} symmetry. But the primary chemical interest is that a well occurs at this geometry and is closer to the conical intersection. As early as 1981, Botschwina *et al.* performed time-of-flight crossed molecular beam experiments on reaction (1) and determined the nonreactive dynamical properties, like the differential quenching cross section and the resulting vibrational energy distribution [2]. Years later, Devivieriedle *et al.* used coherent anti-Stokes Raman scattering (CARS) spectroscopy to measure the vibrational and rotational distribution of H₂ after it quenches the Na(3p) atom [3]. They also found new lines which do not correspond to H₂ lines are observed in the CARS spectrum. Combined with the *ab initio* calculations, the observed lines was attributed to the stabilized exciplex Na(3p)-HH molecule which is formed during the quenching process. More recently, Motzkus *et al.* compared the reactive and quenching behavior of the two different electronically excited sodium atoms Na(3p) and Na(4p) in a collision with H₂ using three different nonlinear optical techniques including CARS, resonance-enhanced CARS, and DFWM (degenerate four-wave mixing). They found the reactive process of reaction (2) is not a direct formation process and involves more than one step [4].

The electronic features and the accumulation of experimental data make NaH₂ system an interesting target for theoretical study. Some pioneering works were performed by semiclassical trajectory method [5-7], and then it has become possible to treat these electronically non-adiabatic processes with accurate quantum dynamics [8,9]. Although these studies provide the final rotational and vibrational energy distributions and the quenching cross sections, most pervious works only focus on unreactive quenching process at low collision energy or the predissociation of the of NaH₂. In this work we calculated the stereodynamics properties of reaction Na(3s) + H₂ → NaH(X¹Σ⁺) + H, and the non-BO effect is also taken into consideration. We compared the non-adiabatic results with the adiabatic quasi-classical trajectory (QCT) calculations. This calculation focus on the impact of the conical intersection on the stereodynamics properties of the state reaction.

Potential energy surfaces and their coupling are the start point of the dynamics studies of a non-adiabatic system. Ben-Nun *et al.* reported a four-state potential energy matrix based on molecular orbital theory and parameterized to *ab initio* calculations. But in this paper we used a two-state potential matrix called Surface set 6 [10], which is based on an eight-state semiempirical diatomics-in-molecules (DIM) potential matrix [4,5]. Surface set 6 has an infinite number of continuous derivatives and is designed to have the correct behavior in the region of the conical intersection. The coherent switching with decay of

mixing (CSDM) algorithm developed by Truhlar and coworkers is used in this work to solve the evolution of the electronic state populations along the semiclassical trajectory. Previously, a natural decay of mixing (NDM) method method is tested for this electronically non-adiabatic system, both reactive and nonreactive, by Hack and Truhlar [11]. The CSDM method develops out of the NDM method and gives more reasonable switching probability [12-14].

This paper is arranged as follows. In Section 2, the CSDM theory for non-adiabatic transitions and the formulas of angular momentum polarization are summarized. Section 3 introduce the potential energy surface applied in this work. Section 4 presents the results of the calculation. The conclusion is presented in Section 5.

2 Theory

2.1 Brief summary of the CSDM method and the algorithm

The coherent switching with decay of mixing method (CSDM) was first proposed by Truhlar and co-workers, they had made elaborate explanations for this method in their early works [12,13]. In this method, the time-dependent electronic Schrodinger equation is employed to describe the electrons coupled with the nucleus motion, and the adiabatic representation as we used in this work can be reduced as

$$\begin{aligned} \dot{\rho}_{kk'} = & \frac{1}{i\hbar} \rho_{kk'} (V_k - V_{k'}) + (\rho_{kk'} - \rho_{k'k'}) \dot{\mathbf{R}} \cdot \mathbf{d}_{kk'} \\ & + \sum_{l \neq k, k'} (\rho_{kl} \dot{\mathbf{R}} \cdot \mathbf{d}_{lk'} - \rho_{lk'} \dot{\mathbf{R}} \cdot \mathbf{d}_{kl}) \end{aligned} \quad (3)$$

where $\rho_{\alpha\beta}$ ($\alpha, \beta = k, k', l$) are elements of the density matrix ρ . k, k' and l denotes different adiabatic electronic states. $\dot{\mathbf{R}}$ is the nuclear velocity. $V_k, V_{k'}$ are the eigenvalues of the electronic Hamiltonian H_{el} , and $\mathbf{d}_{kk'}, \mathbf{d}_{k'l'}$ and $\mathbf{d}_{kl'}$ are non-adiabatic coupling vectors.

The CSDM method introduces decoherence effects to the original SE method by adding decay of mixing terms in the electronic density matrix elements: $\dot{\rho}_{ij} = \dot{\rho}_{ij}^C + \dot{\rho}_{ij}^D$ where the superscript C denotes the coherent contribution and the superscript D denotes the decoherent contribution. The Hamilton equation used to solve the trajectories in phase space also includes the decoherent terms:

$$\begin{aligned} \dot{\mathbf{P}} = & \dot{\mathbf{P}}^C + \dot{\mathbf{P}}^D \\ = & - \sum_k \rho_{kk} \nabla_{\mathbf{R}} V_k + \sum_k \sum_{k'} Re(\rho_{kk'}) (V_k - V_{k'}) \mathbf{d}_{kk'} - \frac{\mu \dot{V}^D}{\mathbf{P} \cdot \hat{\mathbf{s}}} \hat{\mathbf{s}} \end{aligned} \quad (4)$$

$$\dot{\mathbf{R}} = \mathbf{P} / \mu \quad (5)$$

In Eq. (2) the force V^D drives the trajectory to a pure electronic state and the unit vector $\hat{\mathbf{s}}$ is the decoherent direction [13].

The switching probability when the decoherent state switches during the trajectory is obtained by the CSDM-C method [13]:

$$P_{K \rightarrow K'} = \max \left(-\frac{\dot{\tilde{\rho}}_{KK} dt}{\tilde{\rho}_{KK}}, 0 \right) \quad (6)$$

where $\tilde{\rho}_{KK}$ denotes the population when non-adiabatic coupling is strong and $\tilde{\rho}_{KK}$ does not evolve by contributions from the decoherent decay of mixing [12].

2.2 Product rotational polarization

The center-of-mass (CM) frame is used in this work to represent the directional distribution of product's rotational vectors [15]. In this frame, the z-axis is parallel to the reagent relative velocity k , and the y-axis is perpendicular to the plane containing k and k' , where k' is the relative velocity vector of products. j' is the rotational angular momentum of product NaH. The present work focuses on the correlation of the three vectors k , k' and j' and refers to triple-vector correlated angular distribution [16]:

$$P(\theta_r, \phi_r) = \frac{1}{4\pi} \sum_k \sum_{q \geq 0} [a_{q\pm}^k \cos q\phi_r - a_{q\mp}^k \sin q\phi_r] C_{kq}(\phi_r, 0) \quad (7)$$

where C_{kq} is the modified spherical harmonic, θ_r is the angle between j' and k and ϕ_r is the dihedral angle $k' - k - j'$. The polarization parameter a_q^k is given by

$$a_{q\pm}^k = 2 \langle C_{k|q|}(\theta_r, 0) \cos(q\phi_r) \rangle \quad (\text{k is even}) \quad (8)$$

$$a_{q\mp}^k = 2i \langle C_{k|q|}(\theta_r, 0) \sin(q\phi_r) \rangle \quad (\text{k is odd}) \quad (9)$$

$P(\theta_r, \phi_r)$ is expanded up to $k = 7$ as our previous work [17].

3 Potential energy surface and application

The CSDM calculation of $\text{Na} + \text{H}_2$ employs the two coupled diabatic sheets of the 2×2 Surface set 6, where the ground diabatic electronic state U_{11} is correlated with the reaction $\text{Na}(3s) + \text{H}_2 \rightarrow \text{NaH}(A^1\Sigma^+) + \text{H}$ and the first excited diabatic electronic state U_{22} is correlated with the reaction $\text{Na}(3p) + \text{H}_2 \rightarrow \text{NaH}(X^1\Sigma^+) + \text{H}$. The ground adiabatic potential surfaces, which corresponds the reaction $\text{Na}(3s) + \text{H}_2 \rightarrow \text{NaH}(X^1\Sigma^+) + \text{H}$ are obtained by diagonalizing the 2×2 potential matrix. The 3D plots of U_{11} and U_{22} in diabatic PESs with the geometries of $\angle \text{Na-H-H}' = 90^\circ$ are shown in Fig. 1, which is also compared with the ground state adiabatic PES in Fig. 1 (b). The two surfaces in Fig. 1 (a) present the energy path near the reactant and product channels of the two states. The conical intersection occurs at the reacting region before the NaH forms at excited electronic state, it indicates that the reactant $\text{Na}(3s) + \text{H}_2$ would form electronic ground state

NaH product by the contribution of non-adiabatic couplings. Actually NaH($X^1\Sigma^+$) is the main products for both the ground and excited channels since NaH($A^1\Sigma^+$) is unstable. Fig. 1(b) is the ground state adiabatic surface which is used in the QCT calculations. This PES suggests an endothermic type reaction without apparent well or barrier.

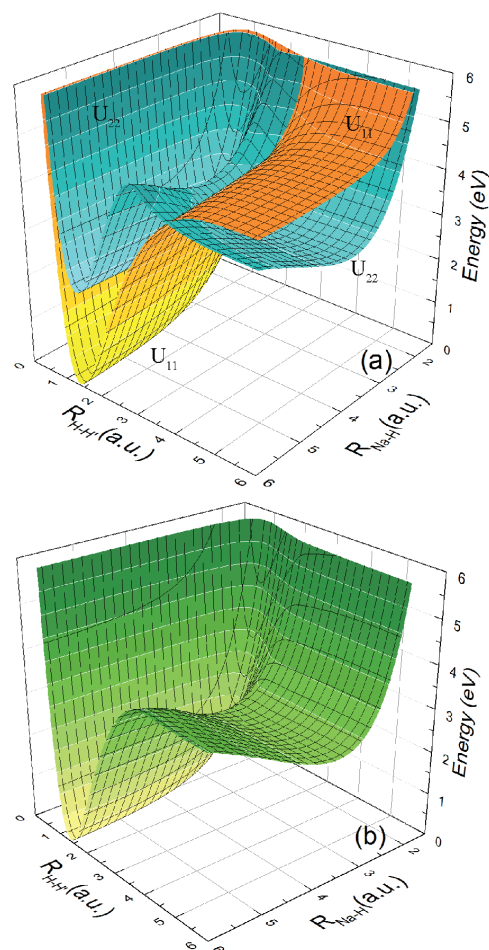


Figure 1: The potential energy surfaces of NaH₂ system in the case of $\angle\text{Na-H-H} = 90^\circ$. (a) U_{11} and U_{22} are in the diabatic representation, (b) the ground state is in the adiabatic representation.

In the CSDM calculations, Monte-Carlo method is used to from the initial state and phase space of the system randomly, for each initial state 100000 trajectories are sampled. To propagation of the phase space, Eq. (2) and Eq. (3) are solved by a sixth order symplectic routine [18,19]. The QCT calculations are performed with the Born-Oppenheimer approximation [17,20-26], so the ground and first excited state adiabatic potential energy surfaces are obtained by diagonalizing the diabatic matrix. For all the reactions discussed in this work, the reactants are initialized with Na (3s) reactant.

4 Results and discussion

Fig. 2 gives the excited function (the integral cross section as a function of collision energy) of reaction $\text{Na}(3s) + \text{H}_2 \rightarrow \text{NaH}(X^1\Sigma^+) + \text{H}$ for the ground rovibrational initial state of H_2 with the collision energy range from 3.5eV to 5.5eV. Both of the QCT and CSDM curves are increased first and then gradually decline after 4.0eV. Seen from the picture, the integral cross sections (ICS) calculated by QCT and CSDM method show the same trend. But it is obvious that the non-BO effect brings smaller cross sections especially at the small and very large collision energy. The shrink of the ICS when considering the non-BO effect suggests that the conical intersection has significant impact on the forming of product NaH, and it is closely related to the structure of the diabatic PES in Fig. 1(a). When the reaction gets the crossing point, parts of the trajectories go through the path on the ground state diabatic surface U_{11} , which corresponds to the unstable high energy product. This channel is almost unreactive, so the non-switching process on U_{11} will certainly decrease the yield of NaH molecular. The “shunting path” on U_{11} may be the most immediate impact of the non-adiabatic cross. However, to form the $\text{NaH}(X^1\Sigma^+)$, the trajectories should switch to the excited state surface U_{22} . This switching is accompanied by strong coupling between the PESs, and the coupling also contributes the shrinking of the ICS.

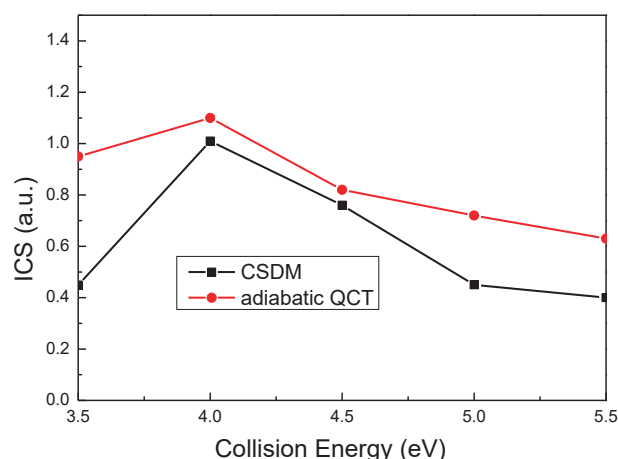


Figure 2: The excitation functions of reaction $\text{Na}(3s) + \text{H}_2 \rightarrow \text{NaH}(X^1\Sigma^+) + \text{H}$ from the adiabatic QCT calculation and non-adiabatic CSDM calculation.

Because the trajectories on U_{11} is non-reactive, the directional distribution of product's rotational angular momentum is mostly affected by the strong coupling between the two states rather than the “shunting path” on U_{11} . The joint distributions of $P(\theta_r, \phi_r)$ calculated by the CSDM method are shown in Fig. 3 for reaction $\text{Na}(3s) + \text{H}_2 \rightarrow \text{NaH}(X^1\Sigma^+)$

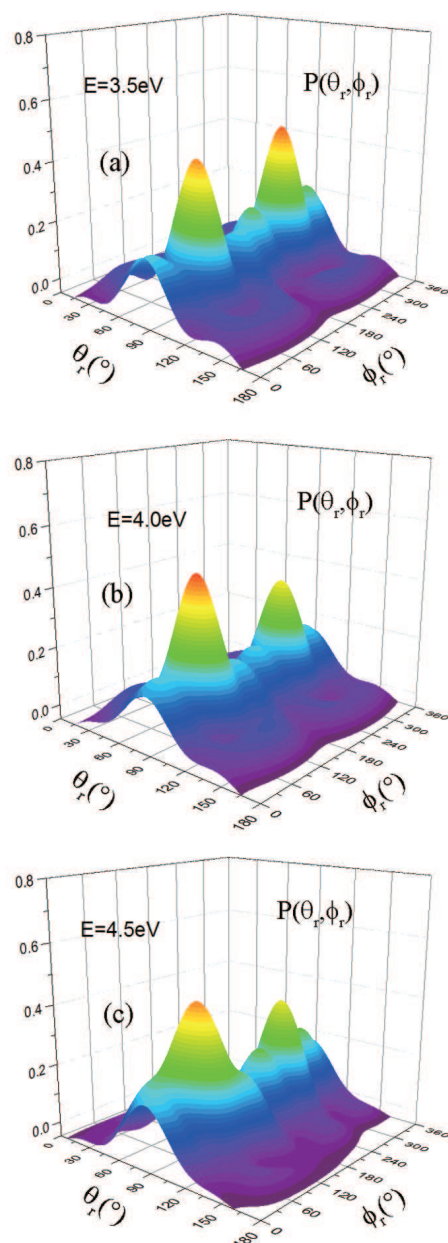


Figure 3: The $P(\theta_r, \phi_r)$ distributions of reaction $\text{Na}(3s) + \text{H}_2 \rightarrow \text{NaH}(X^1\Sigma^+) + \text{H}$ calculated by the CSDM method for three different collision energy; (a) $E=3.5\text{eV}$, (b) $E=4.0\text{eV}$, (c) $E=4.5\text{eV}$.

+ H at three different collision energy. Seen from 3(a), $P(\theta_r, \phi_r)$ shows a strong peak at both $(90^\circ, 90^\circ)$ and $(90^\circ, 270^\circ)$ area, which indicates that the product fragments are ejected with the rotational angular momentum vertical to the k - k' scattering plane. The two peaks

at 3.5 eV show almost symmetrical form, which also indicates that j' is aligned with the y-axis, in spite of the random initial orientation of the reactant molecules in the center of mass (CM) coordinate. But when the collision gets larger, the $P(\theta_r, \phi_r)$ distribution regularly changes as shown from Figs. 3(a)-(c). The peak at $(90^\circ, 270^\circ)$ shows appreciable drop, at the same time the peak at $(90^\circ, 90^\circ)$ almost keeps the same form. This asymmetry of the polarization form indicates that the product fragments are ejected with anticlockwise rotation and j' is tent to be reoriented into the positive direction of y-axis in the CM coordinate. That is, the distribution of NaH's rotational angular momentum will turn from the "alignment" form to the "orientation" form when collision energy increases.

The $P(\theta_r, \phi_r)$ distributions calculated by QCT at the same collision energy are given in Figs. 3(a)-(c). At the collision energy 3.5eV, the distribution also shows a symmetrical form with two strong peaks at $(90^\circ, 90^\circ)$ and $(90^\circ, 270^\circ)$, which indicates that the product fragments are ejected with the rotational angular momentum vertical to the k - k' scattering plane. And when the collision energy increases, the polarization of product in the adiabatic system changes with a similar trend as the diabatic system. The distribution at $(90^\circ, 270^\circ)$ is reduced by the increasing collision energy, but the area $(90^\circ, 90^\circ)$ is enhanced. The whole distribution of product rotational polarization given by QCT calculation also indicates a change from the alignment form to the orientation form, except for the difference that the adiabatic calculation gives more polarized distribution than the diabatic calculation. The distributions shown in Fig. 3 and Fig. 4 suggest that the strong coupling caused by the conical intersection will not change the polarization direction and its distribution mode of product NaH after the switching, but it obviously reduces the intensity of the polarizations.

5 Conclusion

The stereodynamics of reaction $\text{Na}(3s) + \text{H}_2 \rightarrow \text{NaH}(X^1\Sigma^+) + \text{H}$ has been investigated diabatically by the CSDM method. This calculation also compared with the results from the adiabatic QCT calculation. The CSDM calculations are based on the two state diabatic surface set. The comparison of the integral cross sections from the QCT and the CSDM indicates that the conical intersection in the diabatic system will significantly reduce the yield of ground state product $\text{NaH}(X^1\Sigma^+)$. Due to the intersection of the diabatic PES, $\text{Na}(3s) + \text{H}_2$ can also form the excited product $\text{NaH}(A^1\Sigma^+)$, which is unstable. However, the competition of $\text{NaH}(A^1\Sigma^+)$ channel will reduce the cross section of $\text{NaH}(X^1\Sigma^+)$. The joint distribution $P(\theta_r, \phi_r)$, which represents the rotational polarization of products presents a variation from the alignment form at 3.5eV to the orientation form at larger collision energy for both adiabatic and diabatic systems. But the CSDM calculation gives weaker polarized distributions than those in the QCT calculation, which suggests that the conical intersection in the diabatic system will reduce the intensity of the product rotational polarization but will not change the its direction.

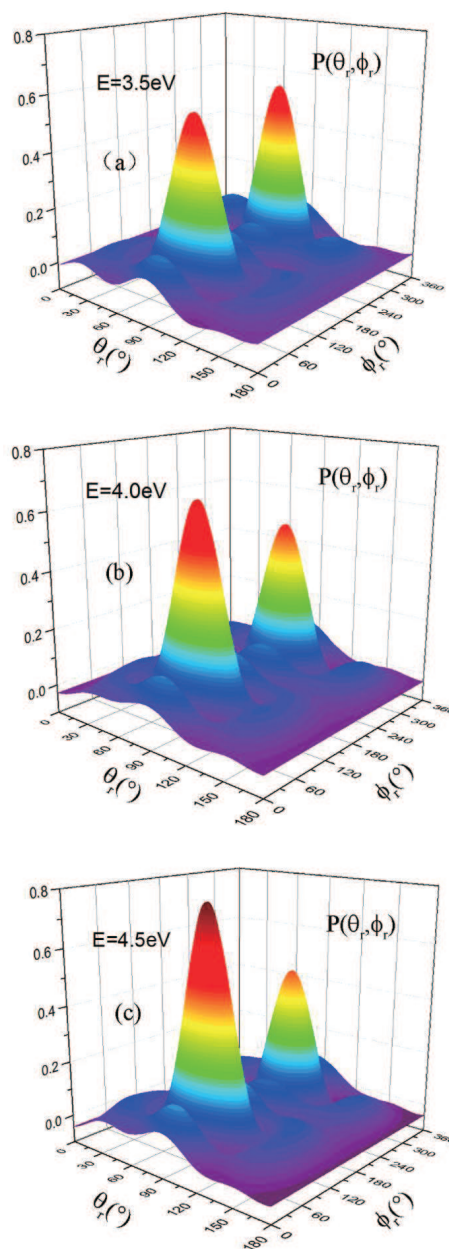


Figure 4: The $P(\theta_r, \phi_r)$ distributions of reaction $\text{Na}(3s) + \text{H}_2 \rightarrow \text{NaH}(X^1\Sigma^+) + \text{H}$ calculated by the adiabatic QCT method for three different collision energy; (a) $E=3.5\text{eV}$, (b) $E=4.0\text{eV}$, (c) $E=4.5\text{eV}$.

Acknowledgments. This work was supported by the National Natural Science Foundation of China (Grant No. 11374045), and Program for New Century Excellent Talents in University (Grant No. NCET-12-0077).

References

- [1] G. J. Tawa, S. L. Mielke, D.G. Truhlar, D. W. Schwenke, J. Chem. Phys. 100 (1994) 5751.
- [2] P. Botschwina, J. Chem. Phys. 75 (11) (1981) 5438.
- [3] R. Devivieriedle, P. Hering, K. L. Kompa, Z. Phys. Chem. 17 (1990) 299.
- [4] M. Motzkus, G. Pichler, K. L. Kompa, P. Hering, J. Chem. Phys. 106 (1997) 9057.
- [5] D. G. Truhlar, J. W. Duff, N. C. Blais, J. C. Tully, B. C. Garrett, J. Chem. Phys. 77 (1982) 764.
- [6] N. C. Blais, D. G. Truhlar, B. C. Garrett, J. Chem. Phys. 78 (1983) 2956.
- [7] N. C. Blais, D. G. Truhlar, J. Chem. Phys. 79 (1983) 1334.
- [8] D. W. Schwenke, S. L. Mielke, G. J. Tawa, R. S. Friedman, P. Halvick, D. G. Truhlar, Chem. Phys. Lett. 203 (1993) 565.
- [9] M. D. Hack, A. W. Jasper, Y. L. Volobuev, D. W. Schwenke, D. G. Truhlar, J. Phys. Chem. A 103 (1999) 6309.
- [10] Y. L. Volobuev, M. D. Hack, M. S. Topaler, D. G. Truhlar, J. Chem. Phys. 112 (2000) 9716.
- [11] M. D. Hack, D. G. Truhlar, J. Chem. Phys. 114 (2001) 9305.
- [12] C. Y. Zhu, A. W. Jasper, D. G. Truhlar, J. Chem. Phys. 120 (2004) 5543.
- [13] C. Y. Zhu, S. Nangia, A. W. Jasper, D. G. Truhlar, J. Chem. Phys. 121 (2004) 7658.
- [14] A. W. Jasper, D. G. Truhlar, J. Chem. Phys. 122 (2005) 44101.
- [15] K. L. Han, G. Z. He, N.Q. Lou, J. Chem. Phys. 105 9 (1996) 8699.
- [16] A. J. Orrewing, R. N. Zare, Annu. Rev. Phys. Chem. 45 (1994) 315.
- [17] D. H. Cheng, J. C. Yuan, M. D. Chen, J. Phys. Chem. A 118 (2014) 55.
- [18] B. Li, T. S. Chu, K.L. Han, J. Comput. Chem. 31 (2010) 362.
- [19] B. Li, K. L. Han, J. Phys. Chem. A 113 (2009) 10189.
- [20] W. Q. Zhang, Y. Z. Li, X. S. Xu, M. D. Chen, Chem. Phys. 367 (2010) 115.
- [21] W. Q. Zhang, S.L. Cong, C.H. Zhang, X. S. Xu, M. D. Chen, J. Phys. Chem. A 113 (2009) 4192.
- [22] L. H. Duan, W. Q. Zhang, X. S. Xu, S. L. Cong, M. D. Chen, Mol. Phys. 107 (2009) 2579.
- [23] J. C. Yuan, D. H. Cheng, M. D. Chen, Rsc Adv. 4 (2014) 36189.
- [24] J. Yuan, D. Cheng, Z. Sun, M. Chen, Mol. Phys. 112 (2014) 2945.
- [25] D. H. Cheng, J. C. Yuan, T. G. Yang, M. D. Chen, Chin. Phys. B 22 (2013) 1674.
- [26] D. Cheng, T. Yang, M. Chen, J Theor. Comput. Chem. 12 (2013) 1250109.